ACS APPLIED MATERIALS & INTERFACES

Research Article

www.acsami.org

A Cationic Diode Based on Asymmetric Nafion Film Deposits

Daping He,[†] Elena Madrid,[†] Barak D. B. Aaronson,[†] Lian Fan,[‡] James Doughty,[‡] Klaus Mathwig,[§] Alan M. Bond,[∥] Neil B. McKeown,[⊥] and Frank Marken*[,†]

[†]Department of Chemistry, University of Bath, Claverton Down, Bath BA2 7AY, U.K.

[‡]Department of Biology and Biochemistry, University of Bath, Claverton Down, Bath BA2 7AY, U.K.

[§]Pharmaceutical Analysis, Groningen Research Institute of Pharmacy, University of Groningen, P.O. Box 196, 9700 AD Groningen, The Netherlands

[∥]Monash University, School of Chemistry, Clayton, Vic 3800, Australia

[⊥]EastChem School of Chemistry, University of Edinburgh, David Brewster Road, Edinburgh, EH9 3FJ, U.K.

ABSTRACT: A thin film of Nafion, of approximately 5 μm thickness, asymmetrically deposited onto a 6 μm thick film of poly(ethylene terephthalate) (PET) fabricated with a 5, 10, 20, or 40 μm microhole, is shown to exhibit prominent ionic diode behavior involving cation charge carrier ("cationic diode"). The phenomenon is characterized via voltammetric, chronoamperometric, and impedance methods. Phenomenologically, current rectification effects are comparable to those observed in nanocone devices where space-charge layer effects dominate. However, for microhole diodes a resistive, a limiting, and an overlimiting potential domain can be identified and concentration polarization in solution is shown to dominate in the closed state.

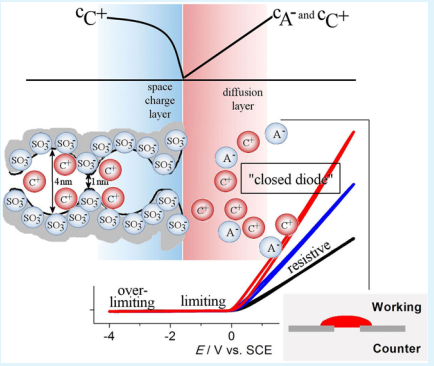

KEYWORDS: *nanofluidics, ion channels, sensor, desalination, ion pump, water*

INTRODUCTION

Ion-conducting nanochannels are present in many microporous materials (membranes) and important technologies based on this class of materials are well established. In contrast, novel devices with individual nanochannels have evolved only recently, inspired by important examples in nature,[1,2] and employed for analytical detection devices[3,4] or in DNA sequencing tools.[5] Devices with a single surface coated nanochannel[6] or a polymer-brush coated nanocone[7] have been observed to give current rectification effects. Engineered materials with many of these nanochannels operating in parallel could be employed in new "blue-energy" harvesting/conversion processes,[8] or in desalination applications.[9] An underlying feature in these types of technologies/devices is a current rectifying ion channel or an "ionic diode".[10] Ionic diodes can be considered also as key components in the emerging field of "iontronics".[11]

Considerable efforts have been made toward the design of current rectifying ion channels, for example based on "track etch" membranes[12] or glass capillaries prepared with nanoscopic precision.[13] Surface functionalization or "active gating" can be employed to control surface charges and to embed the diode functionality into the nanochannel structure.[14] Often conical channels[15] are employed to introduce asymmetry into the device and to define a "bottleneck" point where the diode mechanism is active. Hydrogel embedded into conical channels,[16] also macroscopic hydrogel-hydrogel junctions,[17] have been employed in current rectification and for "ionic transistors".[18,19] Most of these devices are sensitive to ionic strength with higher ionic strength reducing the extent of the double layer and thereby diminishing the magnitude of ion flow rectification phenomenon. We have recently demonstrated that polymer materials with an intrinsically microporous structure are able to give pronounced diode effects when deposited "asymmetrically" onto a microhole. For example, polymers of intrinsic microporosity (or PIMs[20]) have been shown to exhibit "ionic diode" and "ionic flip-flop" effects.[21] In addition, thin films (300 nm) of PIMs have been shown to give strong and pH-switchable ionic diode effects.[22] Similarly, the organometallic framework material ZIF-8 has been suggested for ionic diode applications.[23] Here, we report that a commercial fuoropolymer (Nafion), an intrinsically porous ion-channel containing material, provides excellent current rectification and ionic diode characteristics when fabricated into the appropriate microstructure. A mechanism responsible for the "open" and "closed" diode is proposed.

Nafion (CAS number 66796−30−3) is a well-known commercial ionomer membrane material[24,25] with applications in fuel cells,[26] in catalysis,[27] and in electrolyzers.[28] Nafion self-assembles into a "channel structure"[29,30] that allows cation

Received: February 6, 2017
Accepted: March 13, 2017
Published: March 13, 2017

DOI: 10.1021/acsami.7b01774
ACS Appl. Mater. Interfaces 2017, 9, 11272−11278

transport through sulfonate-lined hydrophilic channels (Figure 1) within a hydrophobic fluorocarbon matrix.[31,32] The negatively charged channels allow permanent uptake and conduction of guest molecules, in particular hydrophobic cations.[33,34]

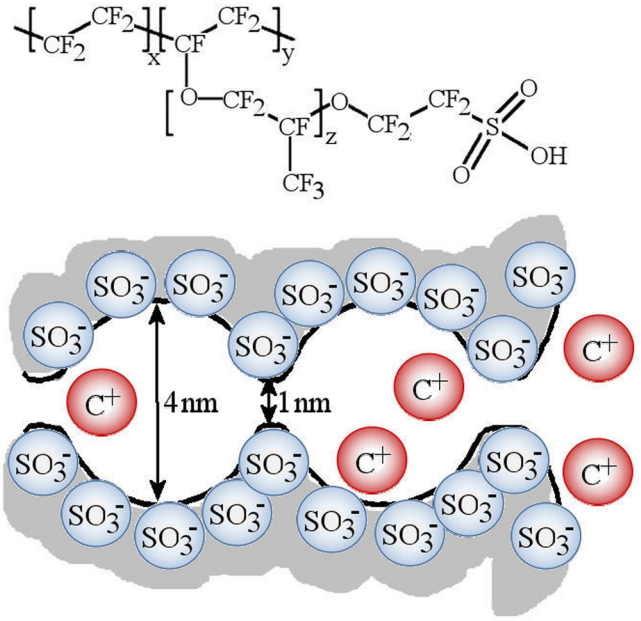

Figure 1. Molecular structure of Nafion and schematic representation of the cation (C^+) transport channel formed via self-assembly.

In this report, Nafion is applied as a thin (approximately 5 μm thick) film onto a microhole in a poly ethylene-terephthalate (PET) substrate. The voltammetric characteristics of the resulting "asymmetric" device are compared to the corresponding "symmetric" case with Nafion applied to both sides of the PET substrate. It is demonstrated that only the "asymmetric" case results in current rectification or ionic diode phenomena. More generally, it is shown that a *macroscopic asymmetry* in the membranelaqueous electrolyte interface on opposite sides of the membrane introduces effects that are usually associated with *microscopically asymmetric* nanocone devices. The physical reasons for the rectification effects are associated with ionomer conductivity in the "open" diode state and with concentration polarization (defined here as a diffusional transport overpotential due to a concentration gradient in the electrolyte) in the external electrolyte close to the PET microhole for the "closed" diode state.

EXPERIMENTAL SECTION

Chemical Reagents. Nafion-117 (5 wt % in a mixture of lower aliphatic alcohols and water), concentrated hydrochloric acid (37%), sodium hydroxide (≥98%), concentrated nitric acid (69.0%), concentrated perchloric acid (70%), sodium chloride, potassium chloride, and rhodamine B (97%) were obtained from Sigma-Aldrich or Fisher Scientific and used without further purification. Solutions were prepared under ambient conditions in volumetric flasks with ultrapure water of resistivity 18.2 MΩ cm from an ELGA Purelab Classic system.

Instrumentation. Electrochemical data (for both voltammetry and impedance) were recorded at $T = 20 \pm 2$ °C on a potentiostated system (Ivium Compactstat). A classic 4-electrode electrochemical cell similar to that employed in previous membrane conductivity studies[35] was used. The membrane separates two tubular half-cells (15 mm diameter), one with the Pt wire working and saturated calomel (SCE) sense electrode (tied together) and the other with the SCE reference and Pt wire counter electrodes (tied together) (see scheme in Figure 2). The cell when assembled has the shape of a "U" and is therefore

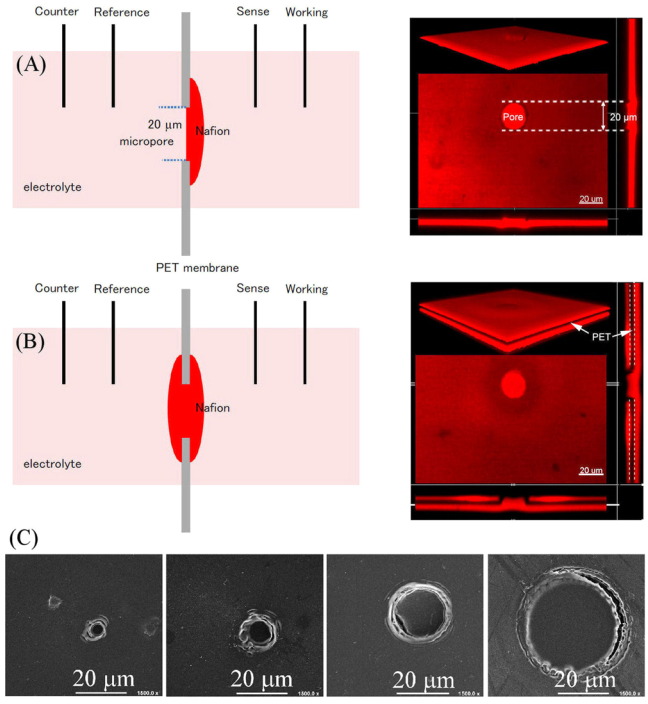

Figure 2. Schematic drawing (not to scale) of the experimental 4-electrode arrangement and fluorescence images for (A) single-sided/asymmetric or (B) double-sided/symmetric Nafion coated (and rhodamine B stained) PET film with 20 μm microhole. Differences in cross-sectional view in top and bottom layer appearance are believed to be linked to light distribution artifacts. (C) SEM images showing PET side for asymmetric Nafion deposits on 40 μm, 20 μm, 10 μm, and 5 μm microholes.

referred to as "U-cell". Fluorescence imaging experiments were performed on a Nikon Eclipse 90i. For fluorescence analysis, rhodamine B was mixed with Nafion-117 (5 wt %) solution to make a solution (approximately 10 μM of rhodamine B), which was then applied to the PET films.

Procedure. In order to form films of Nafion on PET substrates (obtained with 5, 10, 20, 40 μm diameter hole in 6 μm thick PET from Laser-Micro-Machining Ltd., Birmingham, UK), 10 μL Nafion solution was applied to a PET film on a glass substrate (precoated with a thin layer of 1% agarose gel to avoid Nafion passing through the microhole) by solution-casting. With a glass rod the Nafion solution was spread evenly over the PET to give a 1 cm^2 film, which after drying produced a thin uniform coating of typically 5 μm thickness. When peeled off the substrate, asymmetric Nafion deposits on the PET microhole are achieved (see electron micrographs in Figure 2C). For symmetric deposits the deposition was repeated on the opposite side. In order to image the Nafion film fluorescence image stacks were obtained (see Figure 2) for an asymmetric (one-sided) deposit (Figure 2A) and for a symmertic (double-sided) deposit (Figure 2B). In electrochemical measurements with asymmetric deposits the working electrode was always located on the side of the Nafion film.

RESULTS AND DISCUSSION

Nafion Film Microhole Electrochemistry I: Film Characterization. Fluorescence microscopy with rhodamine B stain (Figure 2) reveals the presence of a uniform ~5 μm thick film of Nafion coated over a 20 μm diameter microhole in

DOI: 10.1021/acsami.7b01774
ACS Appl. Mater. Interfaces 2017, 9, 11272−11278

a PET substrate. When the Nafion is applied in two steps from both sides a "sandwich-like" structure is obtained interconnected through the microhole. These sandwich-films are then placed between two electrochemical half-cells (Figure 2) to allow 4-electrode voltammetric measurements.

Figure 3 shows cyclic voltammetry data for the Nafion films. Three cases are shown: (i) PET film with an empty 20 μm

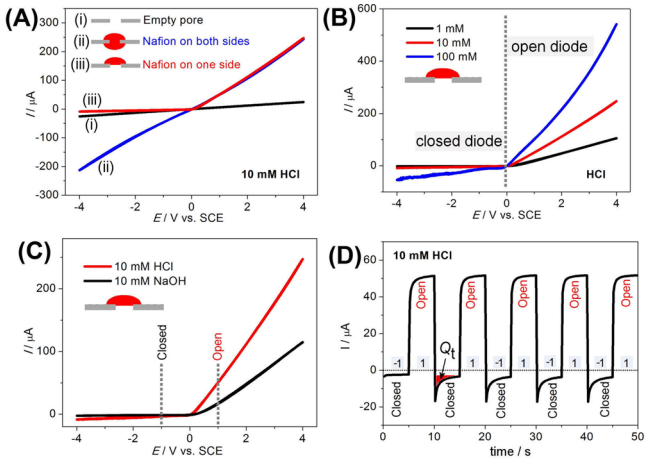

Figure 3. (A) Cyclic voltammograms (scan rate 50 mVs^{-1}) for PET film with a 20 μm diameter microhole in a "U-cell" containing aqueous 10 mM HCl on both sides of the PET film showing results for (i) an empty pore, (ii) symmetrically deposited Nafion, and (iii) asymmetrically deposited Nafion film. (B) Cyclic voltammograms for an asymmetric Nafion film immersed in 1 mM HCl, 10 mM HCl, and 100 mM HCl on both sides of the PET film with rectification ratios 13, 15, 7, respectively. (C) Cyclic voltammograms for an asymmetric Nafion film immersed in 10 mM HCl and in 10 mM NaOH with rectification ratio 15 and 13, respectively. (D) Chronoamperometry data for an asymmetrically deposited Nafion film immersed in 10 mM HCl when switching the potential between −1 V and +1 V.

diameter hole, (ii) a similar film but with Nafion deposited on both sides, and (iii) a similar film but with Nafion deposited only on one side. For data represented in Figure 3A, aqueous 10 mM HCl solutions are present on both sides of the cell. In the absence of Nafion (black line) the currents are dominated by the specific resistivity of the aqueous electrolyte solution filling the pore and a typical "Ohmic" slope with R = 150 kΩ is recorded. With the help of eq 1 for left access, transit, and right access resistivity for a microhole,[36,37] this Ohmic slope can be reconciled with the known specific resistivity of aqueous 10 mM HCl, κ = 0.412 $\Omega^{-1}m^{-1}$.[38]

$$R = \frac{1}{\kappa}\left(\frac{1}{4r} + \frac{L}{\pi r^2} + \frac{1}{4r}\right) \quad (1)$$

In this equation the microhole resistance R is given by the microhole radius, r, the microhole length, L, and the specific conductivity of the electrolyte, κ.

With Nafion applied on both sides (blue line) the current clearly increases due to the locally higher concentration of ionic charge carriers (i.e., protons in Nafion) within the microhole region. The shape of the voltammetric response is again symmetric and dominated by an "Ohmic" slope. With eq 1 the specific resistivity for Nafion can be estimated as κ = 3.6 $\Omega^{-1}m^{-1}$, which seems realistic.[39]

Perhaps interestingly, for the asymmetric case (Figure 3A red line) "ionic diode" or current rectification behavior is observed with a higher current at positive bias (consistent with resistive behavior) and a lower current at negative bias, as compared to the empty hole response (consistent with a limiting behavior). Figure 3B shows data for the asymmetric deposit as a function of the electrolyte concentration. Both, currents in the "closed" state and currents in the "open" state increase with ionic strength. The effects on the near-steady state (or time-independent) current signals due to ionic strength and of microhole size are reported in more detail below.

In Figure 3C, cyclic voltammetry data are shown for both 10 mM HCl and 10 mM NaOH environments. Consistently, ionic diode effects are observed with the "open" state always in the positive potential range. This observation is related to the Nafion structure (in contrast to recent reports of "switching" diode polarity with pH[22]) and ascribed here to the fact that Nafion remains a cation conductor in aqueous HCl (proton transport through Nafion) and in aqueous NaOH (sodium cation transport through Nafion). For both, protons or Na^+ cations, similar effects arise at the Nafion | electrolyte interface with concentration polarization and cation space charge layer effects at the smaller microhole interface linked to the current rectification effect. The higher currents seen for the experiment in 10 mM HCl (compared to currents for 10 mM NaOH) can be explained with the higher proton mobility in Nafion.[40]

With a scan rate of 50 mVs^{-1}, cyclic voltammetry responses appear to be dominated by near-steady state behavior, but there are underlying transient processes that can be revealed, for example, by chronoamperometry. Figure 3D shows typical open/closed transients when switching the ionic diode between +1.0 V and −1.0 V. Transient responses with a typical time constant of approximately 0.1 s (and underlying charge of typically Q_t = 20 μC, see Figure 3D) are observed for both diode opening and diode closing processes. It seems likely that the transient component of the current response is mainly associated with transport of cations, which could imply formation of either a "polymer space charge region" or a "solution concentration polarization region" resulting in the closed diode state. Nafion has a density of approximately 1.67 g cm^{-3}[40] and a molecular mass of approximately 1100 g per mol of sulfonate functional group. For a "plug" of 20 μm diameter and 5 μm length this amounts to a weight of 2.6 ng and therefore a charge of 2.4 pmol (= 0.23 μC). The observed transient charge during switching is 2 orders of magnitude higher and therefore more likely to be associated with concentration polarization in solution. For a microelectrode concentration polarization should result in an estimated time constant of roughly $\tau = r^2/D$ or here approximately 0.1 s, consistent with the experiment.

An alternative approach to the characterization of transient phenomena is based on electrochemical impedance spectroscopy. Figure 4 shows impedance data for (A) the PET film with empty microhole, (B) the symmetric Nafion deposit, and (C) the asymmetric Nafion deposit. For the empty microhole, a voltage-independent spectrum is obtained with a classic semicircle indicative of RC-parallel behavior. In fact the equivalent circuit shown as inset in Figure 4A can be employed to fit the data to give R1 = 1.3 kΩ (consistent with bulk solution resistance), R2 = 148 kΩ (consistent with only microhole and access region resistance, see eq 1), and C = 0.8 nF (consistent with PET film capacitance).

Figure 4B shows impedance spectroscopy data for the PET microhole coated symmetrically with Nafion. Again a potential independent impedance is observed with give R1 = 0.9

DOI: 10.1021/acsami.7b01774
ACS Appl. Mater. Interfaces 2017, 9, 11272−11278

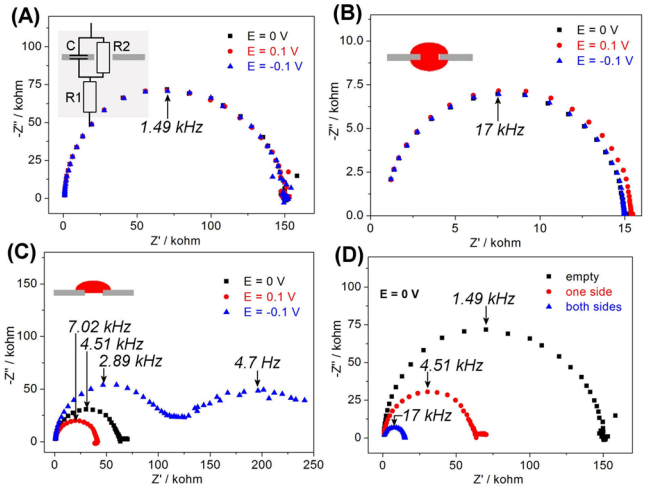

Figure 4. Electrochemical impedance data (frequency range 100 kHz to 1 Hz; amplitude) for a 20 μm diameter pore in PET immersed into 10 mM HCl on both sides compared to data obtained with symmetric and with asymmetric Nafion deposits. Data are shown for (A) the PET microhole without Nafion, (B) the microhole with Nafion applied to both sides, (C) the microhole with Nafion applied to only one side, and (D) a comparison of empty, one sided, and two-sided Nafion for an applied voltage of 0 V.

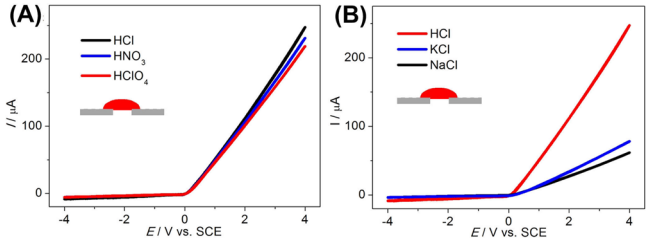

Figure 5. (A) Cyclic voltammograms (scan rate 50 mVs^{-1}) for an asymmetric Nafion membrane immersed on both sides with aqueous 10 mM HCl, HNO_3, or $HClO_4$ with rectification ratios 15, 19, 19, respectively. (B) As above, but with 10 mM HCl, KCl, and NaCl with rectification ratios 15, 9, 13, respectively.

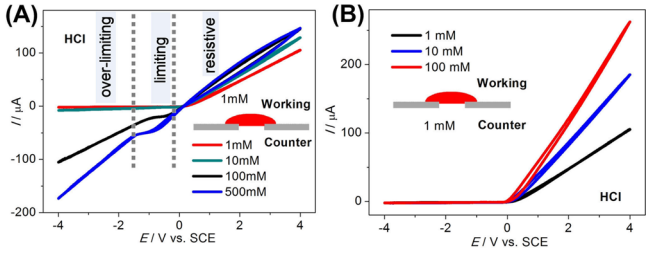

Figure 6. (A) Cyclic voltammograms (scan rate 50 mVs^{-1}) for an asymmetric Nafion membrane immersed on the working electrode sides in 1 mM HCl and on the counter electrode side with 1, 10, 100, 1000 mM HCl. (B) As above, but with 1 mM HCl at the counter electrode side and 1, 10, 100 mM (with rectification ratios 31, 18, 13, respectively) at the working electrode side.

kΩconsistent with bulk resistance for both aqueous solution and the polymer region outside the access region), R2 = 14 kΩ (consistent with microhole and access Nafion resistance within the polymer), and C = 0.7 nF (consistent with PET film capacitance). Figure 4C shows data for the asymmetrically deposited Nafion film and for this case clear changes in impedance as a function of applied potential are noted. The high frequency semicircle remains (for −0.1/0.0/0.1 V applied potential, respectively) with R1 = 0.18/0.83/1.3 kΩ and C = 0.6 nF at all three potentials. Parameter R2 = 99/63/40 kΩ mostly reflects the internal resistance in the Nafion film, which appears to go down when the diode "opens". Intriguingly, a second nonideal semicircle is observed (Figure 4C) with a time constant of approximately 0.1 s order of magnitude, consistent with transient phenomena during opening/closing processes of the ionic diode. This time constant is proposed to be again associated with concentration polarization.

Nafion Film Microhole Electrochemistry II: Anion versus Cation Effects. The effect of anions and cations are investigated, as well as ionic strength imbalances in left and right half-cells, in order to better understand "cationic diode" processes of the Nafion asymmetrically deposited onto microhole-containing PET film. Figure 5A shows cyclic voltammetry data for aqueous 10 mM acids: HCl, HNO_3, and $HClO_4$. For the asymmetrically deposited Nafion film, reproducible diodes (current rectifiers) are observed in all three cases. The effect of chloride, nitrate, or perchlorate anions remain insignificant.

In contrast, when investigating the effect of the electrolyte cation, much more obvious changes in diode behavior are observed (Figure 5B). Currents for the open diode are considerably higher in the presence of protons compared to those for Na^+ or K^+. This is consistent with a higher mobility for protons relative to Na^+ and K^+. Values for ion diffusivity within Nafion[41] in the presence of 1 mol dm^{-3} aqueous chloride solution have been reported as $D(H^+)$ = 5.3 × 10^{-10} m^2 s^{-1}, $D(Na^+)$ = 1.58 × 10^{-10} m^2 s^{-1}, $D(K^+)$ = 0.86 × 10^{-10} m^2 s^{-1}, and for lower salt concentrations $D(Na^+) \approx D(K^+)$. This trend is in good agreement with the current−potential data shown in Figure 5B. The mobility of cations in the Nafion film deposit appears to be crucial in determining the magnitude of the current in the open diode state.

When changing asymmetrically the supporting electrolyte concentration, there are two cases to consider. Figure 6A shows data for cyclic voltammograms employing an aqueous 1 mM HCl solution on the side of the Nafion membrane while changing the aqueous electrolyte from 1 mM, 10 mM, 100 mM, to 500 mM on the opposite side of the PET microhole. It can be observed that the closed state of the diode is strongly affected with almost complete "opening" at 500 mM HCl. The current response in the "open" state of the diode remains largely unaffected. It can be concluded that the "closed" state of the diode is due mainly to a region close to the small area Nafion | electrolyte interface in the vicinity of the PET microhole. This region can be identified as the concentration polarization region in the electrolyte solution close to the microhole. Yossifon and coworkes[42−45] and Chang[46] have shown that for nanoslot channels external concentration polarization causes a "limiting" region where current is limited by an electroneutral diffusion−migration layer similar to that observed at microelectrodes under conditions of no added supporting electrolyte.[47] This can be compared to the concentration polarization case here. For HCl as a 1:1 electrolyte it is possible to contrast to the literature concentration polarization case of 1:1 ferricenium salt reduction at a metal microelectrode without added electrolyte. At the metal electrode the diffusion−migration transport is linked to electron transfer, whereas at the diode the diffusion−migration transport is linked to cation flux through the Nafion layer. The

DOI: 10.1021/acsami.7b01774
ACS Appl. Mater. Interfaces 2017, 9, 11272−11278

expected mass transport limited current[48] is $I_{lim} = Z \times 4\ FDrc$ (with $Z = 2$ for a 1:1 electrolyte, F, the Faraday constant, D the diffusion coefficient, r the microdisc radius, and c the concentration). Assuming D_{proton}[49] $= 9 \times 10^{-9}$ m^2s^{-1}, the estimated limiting current is $I_{lim} = 35$ μA, which is not too far from the observed value $I_{lim} = 50$ μA (see Figure 6A, "limiting region"). Therefore, following on Yossifon's work, the "limiting region" as well as the "resistive region" and the "over-limiting region" (caused by convection[50]) can be identified. For Nafion asymmetrically deposited onto a microhole the closed state of the ionic diode is dominated by concentration polarization in solution.

In the case of the asymmetrically deposited Nafion, equal concentrations of HCl on both sides of the membrane, and a closed state, the high resistivity in the "limiting" or "over-limiting" regime is therefore determined by the concentration polarization (i.e., cation depletion occurs with a gradient of C^+ and A^- concentrations in the diffusion layer while maintaining electroneutrality) on the microhole side of the Nafion membrane. The reduced conductivity close to the PET microhole caused by concentration polarization (i.e., small number of ions) limits/determines the overall current.

Data shown in Figure 6B demonstrate the complementary case of varying the aqueous electrolyte concentration in the half-cell facing the Nafion film from 1 mM, 10 mM, to 100 mM. In this case the "closed" state of the diode (negative potential range) is unaffected and only the "open" state of the diode (positive potential range) is seen to significantly increase in current with increasing HCl concentration. The increase in current is not linear with aqueous solution concentration and may be linked to some additional partitioning of HCl into the Nafion film (affecting the proton mobility in the Nafion). In addition to the nature of cation and anion and the electrolyte concentration effects, it is of interest to explore microhole size/geometry effects on the diode characteristics.

Nafion Film Microhole Electrochemistry III: Microhole Size Effects. Experiments were performed with a ~5 μm thick Nafion film deposited onto laser-drilled PET films of a systematically increasing diameter (see Figure 2C). Cyclic voltammetry data in Figure 7 demonstrate the diode effect for

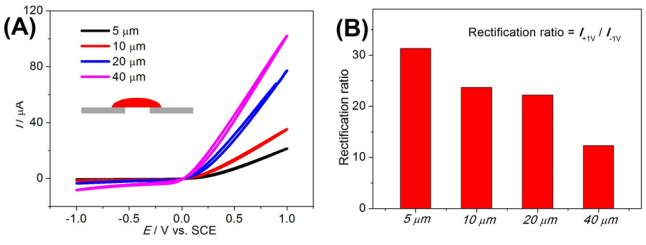

Figure 7. (A) Cyclic voltammograms (scan rate 50 mV s^{-1}) in 10 mM HCl and for 5, 10, 20, and 40 μm diameter microhole in a 6 μm thick PET film coated asymmetrically with Nafion. (B) Bar graph for the current rectification ratio at ±1 V versus microhole diameter.

10 mM HCl (in both half-cells) for 5, 10, 20, and 40 μm diameter microholes. As expected, the increase in diameter causes an increase in the currents for both open and closed diode. However, the currents do not scale with area. The relative change in current magnitude for open and closed states shows a pattern indicative of a slightly better current rectification at smaller microholes. The diameter of the microhole is an important parameter in controlling ionic diode characteristics, but other parameters such as Nafion film thickness and PET film thickness may be equally important and will require further study.

Comparing the present data for Nafion on a microhole to previous studies of nanocone ion current rectification processes is possible, if we assume Nafion to be composed of many nanochannels. Asymmetry for the nanocone is introduced at microscopic level at the interface to the electrolyte solution. Asymmetry for the Nafion films is introduced at macroscopic level due to the difference in area exposed to the opposing electrolyte solutions and the difference in diffusion−migration access to the microhole. Nanocone effects are based on double layer phenomena (formation of a space charge layer or accumulation-depletion[51]), which also lead to changes in the apparent activation energy for ion transport[52] in these devices. The accumulation-depletion model has been developed by White and co-workers[53,54] and has been employed to account for current rectification in single cone nanochannels. A variation of the ion concentration in the vicinity of the cone-tip to solution phase interface has been identified as the prime reason for local changes in ion conductivity that give rise to the current rectification effect. Here, for Nafion, the role of the asymmetric cone shape for a single channel is replaced by the asymmetry in the Nafion microhole deposit exposed to the electrolyte solution phase. The effect of the space charge layer is complemented by the concentration polarization phenomenon in solution. In fact, for the highly cation-conductive Nafion the concentration polarization phenomenon dominates. In a qualitative manner, the field applied externally to the Nafion film can be suggested to

(A) drop across the whole Nafion film for the "***open diode***" with film resistivity (mainly in the access resistance region close to and within the microhole) dominating the current flow and

(B) drop primarily across the small Nafion | electrolyte interface within the microhole for the "***closed diode***" associated with a space charge layer and with concentration polarization in the solution phase, which leads to loss of electrolyte and conductivity (depletion) locally in the interfacial region;

(C) for the case of Nafion the high ionic conductivity in the polymer and the high concentration of mobile cations in the polymer cause concentration polarization in the electrolyte close to the microhole to dominate the resistivity in the "closed" state.

Figure 8 shows a schematic drawing to summarize the conditions at the Nafion | electrolyte interface for the closed diode. The concentration of cations in both adjacent electrolyte solution and Nafion film approach zero. In the "over-limiting" state additional convective phenomena arise. In the "resistive" or "open" state, the Nafion film resistance limits current flow. In future, further quantitative modeling based on Poisson-Nernst-Plank methods (while taking into account the geometry of the Nafion on PET) will be necessary to confirm these ideas and to allow quantitative prediction of device performance for example in desalination or in energy conversion.

CONCLUSION

It has been shown that asymmetry in the deposition of an ion-nanochannel material, such as commercial Nafion 117, can be used to induce current rectification phenomena or ionic diode effects. In this particular case a "cationic diode" has been

DOI: 10.1021/acsami.7b01774
ACS Appl. Mater. Interfaces 2017, 9, 11272−11278

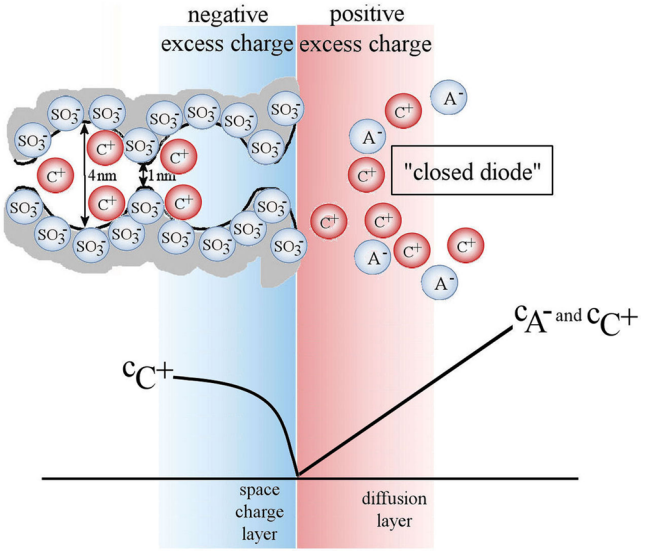

Figure 8. Schematic depiction (not to scale) of the "closed" Nafion | aqueous electrolyte interface within the microhole and of the effect of the interfacial polarization (presence of excess charge) with concentration polarization in the diffusion layer and cation concentration approaching zero at the interface.

produced with effective rectification for many types of cations. The polymer | electrolyte interface in the microhole provides the key to current rectification effects with currents for "open" diodes being dominated by ionomer conductivity and currents for "closed" diodes being dominated by external concentration polarization in the electrolyte. Smaller microholes have been shown to produce improved current rectification and are likely to allow faster diode switching times.[55]

In future, many other semipermeable materials should become available for the development of improved microhole current rectification devices. Both "cationic diodes" and "anionic diodes" as well as ion-selective diodes are possible. Particularly interesting is the prospect for chemical modification of the ionomer | electrolyte interface to provide switchable or pH sensitive devices.[56] Applications could be possible in biomimetic ion gates,[57] biosensors,[58] photoresponsive ion gates,[59] stimuli-response gates,[60] or in "ionic sensors" which are devoid of immediate metal components and are based entirely on ion conductors in the sensing mechanism.

AUTHOR INFORMATION

Corresponding Author

*E-mail f.marken@bath.ac.uk.

ORCID

Frank Marken: 0000-0003-3177-4562

Funding

EPSRC (EP/K004956/1) and Leverhulme Foundation (RPG-2014−308).

Notes

The authors declare no competing financial interest.

ACKNOWLEDGMENTS

D.H. thanks the Royal Society for a Newton International Fellowship. E.M. thanks EPSRC (EP/K004956/1) and A.B. is grateful for support from the Leverhulme Foundation (RPG-2014-308: "New Materials for Ionic Diodes and Ionic Photodiodes").

REFERENCES

(1) Zhang, H. C.; Tian, Y.; Jiang, L. Fundamental Studies and Practical Applications of Bio-inspired Smart Solid-State Nanopores and Nanochannels. *Nano Today* **2016**, *11*, 61−81.

(2) Guo, W.; Tian, Y.; Jiang, L. Asymmetric Ion Transport through Ion-Channel-Mimetic Solid-State Nanopores. *Acc. Chem. Res.* **2013**, *46*, 2834−2846.

(3) Slouka, Z.; Senapati, S.; Chang, H. C. Microfluidic Systems with Ion-Selective Membranes. *Annu. Rev. Anal. Chem.* **2014**, *7*, 317−335.

(4) Miles, B. N.; Ivanov, A. P.; Wilson, K. A.; Dogan, F.; Japrung, D.; Edel, J. B. Single Molecule Sensing with Solid-State Nanopores: Novel Materials, Methods, and Applications. *Chem. Soc. Rev.* **2013**, *42*, 15−28.

(5) Ying, Y. L.; Cao, C.; Long, Y. T. Single Molecule Analysis by Biological Nanopore Sensors. *Analyst* **2014**, *139*, 3826−3835.

(6) Hu, N.; Ai, Y.; Qian, S. Z. Field Effect Control of Electrokinetic Transport in Micro/Nanofluidics. *Sens. Actuators, B* **2012**, *1161*, 1150−1167.

(7) Lin, J. Y.; Lin, C. Y.; Hsu, J. P.; Tseng, S. Ionic Current Rectification in a pH-Tunable Polyelectrolyte Brushes Functionalized Conical Nanopore: Effect of Salt Gradient. *Anal. Chem.* **2016**, *88*, 1176−1187.

(8) Jia, Z. J.; Wang, B. G.; Song, S. Q.; Fan, Y. S. Blue Energy: Current Technologies for Sustainable Power Generation from Water Salinity Gradient. *Renewable Sustainable Energy Rev.* **2014**, *31*, 91−100.

(9) Madrid, E.; Cottis, P.; Rong, Y. Y.; Rogers, A. T.; Stone, J. M.; Malpass-Evans, R.; Carta, M.; McKeown, N. B.; Marken, F. Water Desalination Concept Using an Ionic Rectifier Based on a Polymer of Intrinsic Microporosity (PIM). *J. Mater. Chem. A* **2015**, *3*, 15849−15853.

(10) Koo, H. J.; Velev, O. D. Ionic Current Devices-Recent Progress in the Merging of Electronic, Microfluidic, and Biomimetic Structures. *Biomicrofluidics* **2013**, *7*, 031501.

(11) Chung, H. G.; Dong, T. Iontronics. *Annu. Rev. Anal. Chem.* **2015**, *8*, 441−462.

(12) Cheng, L. J.; Guo, L. J. Nanofluidic Diodes. *Chem. Soc. Rev.* **2010**, *39*, 923−938.

(13) Liu, Y. F.; Yobas, L. Cylindrical Glass Nanocapillaries Patterned via Coarse Lithography (> 1 μm) for Biomicrofluidic Applications. *Biomicrofluidics* **2012**, *6*, 046502.

(14) Bearden, S.; Simpanen, E.; Zhang, G. G. Active Current Gating in Electrically Biased Conical Nanopores. *Nanotechnology* **2015**, *26*, 185502.

(15) Xiao, K.; Xie, G. H.; Zhang, Z.; Kong, X. Y.; Liu, Q.; Li, P.; Wen, L. P.; Jiang, L. Enhanced Stability and Controllability of an Ionic Diode Based on Funnel-Shaped Nanochannels with an Extended Critical Region. *Adv. Mater.* **2016**, *28*, 3345−3350.

(16) Wang, L. L.; Zhang, H. C.; Yang, Z.; Zhou, J. J.; Wen, L. P.; Li, L.; Jiang, L. Fabrication of Hydrogel-Coated Single Conical Nanochannels Exhibiting Controllable Ion Rectification Characteristics. *Phys. Chem. Chem. Phys.* **2015**, *17*, 6367−6373.

(17) Hegedus, L.; Noszticzius, Z.; Papp, A.; Schubert, A. P.; Wittmann, M. Polarization Phenomena in Hydrogel Membranes - Experimental Realization of an Electrolyte Diode. *ACH-Models in Chem.* **1995**, *132*, 207−224.

(18) Hegedus, L.; Kirschner, N.; Wittmann, M.; Noszticzius, Z. Electrolyte Transistors: Ionic Reaction-Diffusion Systems with Amplifying Properties. *J. Phys. Chem. A* **1998**, *102*, 6491−6497.

(19) Sun, G.; Senapati, S.; Chang, H. C. High-Flux Ionic Diodes, Ionic Transistors and Ionic Amplifiers Based on External Ion Concentration Polarization by an Ion Exchange Membrane: a new Scalable Ionic Circuit Platform. *Lab Chip* **2016**, *16*, 1171−1177.

(20) McKeown, N. B.; Budd, P. M. Exploitation of Intrinsic Microporosity in Polymer-Based Materials. *Macromolecules* **2010**, *43*, 5163−5176.

(21) Madrid, E.; Rong, Y. Y.; Carta, M.; McKeown, N. B.; Malpass-Evans, R.; Attard, G. A.; Clarke, T. J.; Taylor, S. H.; Long, Y. T.; Marken, F. Metastable Ionic Diodes Derived from an Amine-Based

DOI: 10.1021/acsami.7b01774
ACS Appl. Mater. Interfaces 2017, 9, 11272−11278

Polymer of Intrinsic Microporosity. *Angew. Chem., Int. Ed.* **2014**, *53*, 10751−10754.
(22) Rong, Y. Y.; Song, Q.; Mathwig, K.; Madrid, E.; He, D.; Niemann, R. G.; Cameron, P. J.; Dale, S. E. C.; Bending, S.; Carta, M.; Malpass-Evans, R.; McKeown, N. B.; Marken, F. pH-Induced Reversal of Ionic Diode Polarity in 300 nm Thin Membranes Based on a Polymer of Intrinsic Microporosity. *Electrochem. Commun.* **2016**, *69*, 41−45.
(23) Madrid, E.; Buckingham, M. A.; Stone, J. M.; Rogers, A. T.; Gee, W. J.; Burrows, A. D.; Raithby, P. R.; Celorrio, V.; Fermin, D. J.; Marken, F. Ion Flow in a Zeolitic Imidazolate Framework Results in Ionic Diode Phenomena. *Chem. Commun.* **2016**, *52*, 2792−2794.
(24) Mauritz, K. A.; Moore, R. B. State of Understanding of Nafion. *Chem. Rev.* **2004**, *104*, 4535−4585.
(25) Leddy, J. Modification of Nafion on Membranes: Tailoring Properties for Function. *ACS Symp. Ser.* **2015**, *1213*, 99−133.
(26) Cele, N.; Ray, S. S. Recent Progress on Nafion-Based Nanocomposite Membranes for Fuel Cell Applications. *Macromol. Mater. Eng.* **2009**, *294*, 719−738.
(27) Olah, G. A.; Iyer, P. S.; Prakash, G. K. S. Perfluorinated Resinsulfonic Acid (Nafion-H) Catalysis in Synthesis. *Synthesis* **1986**, *7*, 513−531.
(28) Ito, H.; Maeda, T.; Nakano, A.; Takenaka, H. Properties of Nafion Membranes under PEM Water Electrolysis Conditions. *Int. J. Hydrogen Energy* **2011**, *36*, 10527−10540.
(29) Ling, X.; Bonn, M.; Parekh, S. H.; Domke, K. F. Nanoscale Distribution of Sulfonic Acid Groups Determines Structure and Binding of Water in Nafion Membranes. *Angew. Chem., Int. Ed.* **2016**, *55*, 4011−4015.
(30) Hsu, W. Y.; Barkley, J. R.; Meakin, P. Ion Percolation and Insulator-to-Conductor Transition in Nafion Perfluorosulfonic Acid Membranes. *Macromolecules* **1980**, *13*, 198−200.
(31) Davis, T. A.; Pletcher, J. D.; Genders, D. *Ion Permeable Membranes*; The Electrochemical Consultancy: Hants, UK, 1997.
(32) Leddy, J. *Nanomaterials for Sustainable Energy*. In ACS Symposium Series; Liu, J. L.; Bashir, S., Eds.; ACS: New York, 2015; Vol. *1213*, pp 99−133.
(33) Milsom, E. V.; Novak, J.; Green, S. J.; Zhang, X. H.; Stott, S. J.; Mortimer, R. J.; Edler, K.; Marken, F. Layer-by-layer Deposition of Open-Pore Mesoporous TiO_2-Nafion Film Electrodes. *J. Solid State Electrochem.* **2007**, *11*, 1109−1117.
(34) Azad, U. P.; Yadav, D. K.; Ganesan, V.; Marken, F. Hydrophobicity Effects in Iron Polypyridyl Complex Electrocatalysis within Nafion Thin-Film Electrodes. *Phys. Chem. Chem. Phys.* **2016**, *18*, 23365−23373.
(35) Slade, S. M.; Ralph, T. R.; Ponce de León, C.; Campbell, S. A.; Walsh, F. C. The Ionic Conductivity of a Nafion 1100 Series of Proton-exchange Membranes Re-cast from Butan-1-ol and Propan-2-ol. *Fuel Cells* **2010**, *10*, 567−574.
(36) Hall, J. E. Access Resistance of a Small Circular Pore. *J. Gen. Physiol.* **1975**, *66*, 531−532.
(37) Luan, B. Q. Numerically Testing Phenomenological Models for Conductance of a Solid-State Nanopore. *Nanotechnology* **2015**, *26*, 055502.
(38) Lide, R. *Handbook of Chemistry and Physics*, 74th ed.; CRC Press: London, 1993.
(39) Saab, A. P.; Garzon, F. H.; Zawoszinski, T. A. The Effects of Processing Conditions and Chemical Composition on Electronic and Ionic Resistivities of Fuel Cell Electrode Composites. *J. Electrochem. Soc.* **2003**, *150*, A214−A218.
(40) Stenina, I. A.; Sistat, P.; Rebrov, A. I.; Pourcelly, G.; Yaroslavtsev, A. B. Ion Mobility in Nafion-117 Membranes. *Desalination* **2004**, *170*, 49−57.
(41) Zook, L. A.; Leddy, J. Density and Solubility of Nafion: Recast, Annealed, and Commercial Films. *Anal. Chem.* **1996**, *68*, 3793−3796.
(42) Yossifon, G.; Mushenheim, P.; Chang, H. C. Controlling Nanoslot Overlimiting Current with the Depth of a Connecting Microchamber. *EPL* **2010**, *90*, 64004.
(43) Yossifon, G.; Mushenheim, P.; Chang, Y. C.; Chang, H. C. Nonlinear Current-Voltage Characteristics of Nanochannels. *Phys. Rev. E* **2009**, *79*, 046305.
(44) Yossifon, G.; Mushenheim, P.; Chang, Y. C.; Chang, H. C. Eliminating the Limiting-Current Phenomenon by Geometric Field Focusing into Nanopores and Nanoslots. *Phys. Rev. E* **2010**, *81*, 046301.
(45) Chang, H. C.; Yossifon, G.; Demekhin, E. A. Nanoscale Electrokinetics and Microvortices: How Microhydrodynamics Affects Nanofluidic Ion Flux. In *Annual Review of Fluid Mechanics*; Davis, S. H., Moin, P., Eds.; Annual Reviews: Palo Alto, 2012; Vol. *44*; pp 401−426.
(46) Sun, G.; Senapati, S.; Chang, H. C. High-Flux Ionic Diodes, Ionic Transistors and Ionic Amplifiers Based on External Ion Concentration Polarization by an Ion Exchange Membrane: a New Scalable Ionic Circuit Platform. *Lab Chip* **2016**, *16*, 1171−1177.
(47) Bond, A. M. Past, Present and Future Contributions of Microelectrodes to Analytical Studies Employing Voltammetric Detection - a Review. *Analyst* **1994**, *119*, R1−R21.
(48) Cooper, J. B.; Bond, A. M.; Oldham, K. B. Microelectrode Studies without Supporting Electrolyte - Model and Experimental Comparison for Singly and Multiply Charged Ions. *J. Electroanal. Chem.* **1992**, *331*, 877−895.
(49) Weber, J.; Wain, A. J.; Marken, F. Microwire Chronoamperometric Determination of Concentration, Diffusivity, and Salinity for Simultaneous Oxygen and Proton Reduction. *Electroanalysis* **2013**, *27*, 1829−1835.
(50) Rubinstein, I.; Zaltzman, B. Electro-osmotic Slip of the Second Kind and Instability in Concentration Polarization at Electrodialysis Membranes. *Math. Models Methods Appl. Sci.* **2001**, *11*, 263−300.
(51) Siwy, Z. S. Ion-Current Rectification in Nanopores and Nanotubes with Broken Symmetry. *Adv. Funct. Mater.* **2006**, *16*, 735−746.
(52) Perera, R. T.; Johnson, R. P.; Edwards, M. A.; White, H. S. Effect of the Electric Double Layer on the Activation Energy of Ion Transport in Conical Nanopores. *J. Phys. Chem. C* **2015**, *119*, 24299−24306.
(53) White, H. S.; Bund, A. Ion Current Rectification at Nanopores in Glass Membranes. *Langmuir* **2008**, *24*, 2212−2218.
(54) Kubeil, C.; Bund, A. The Role of Nanopore Geometry for the Rectification of Ionic Currents. *J. Phys. Chem. C* **2011**, *115*, 7866−7873.
(55) Aaronson, B. D. B.; He, D.; Madrid, E.; Johns, M. A.; Scott, J. L.; Fan, L.; Doughty, J.; Kadowaki, M. A. S.; Polikarpov, I.; McKeown, N. B.; Marken, F. Ionic Diodes Based on Regenerated α-Cellulose Films Deposited Asymmetrically onto a Microhole. *ChemistrySelect* **2017**, *2*, 871−875.
(56) Wen, L. P.; Xiao, K.; Sainath, A. V. S.; Komura, M.; Kong, X. Y.; Xie, G. H.; Zhang, Z.; Tian, Y.; Iyoda, T.; Jiang, L. Engineered Asymmetric Composite Membranes with Rectifying Properties. *Adv. Mater.* **2016**, *28*, 757−763.
(57) Liu, Q.; Xiao, K.; Wen, L. P.; Lu, H.; Liu, Y. H.; Kong, X. Y.; Xie, G. H.; Zhang, Z.; Bo, Z. S.; Jiang, L. Engineered Ionic Gates for Ion Conduction Based on Sodium and Potassium Activated Nanochannels. *J. Am. Chem. Soc.* **2015**, *137*, 11976−11983.
(58) Ali, M.; Nasir, S.; Ensinger, W. Bioconjugation-Induced Ionic Current Rectification in Aptamer-Modified Single Cylindrical Nanopores. *Chem. Commun.* **2015**, *51*, 3454−3457.
(59) Xiao, K.; Kong, X. Y.; Zhang, Z.; Xie, G. H.; Wen, L. P.; Jiang, L. Construction and Application of Photoresponsive Smart Nanochannels. *J. Photochem. Photobiol., C* **2016**, *26*, 31−47.
(60) Xiao, K.; Xie, G. H.; Li, P.; Liu, Q.; Hou, G. L.; Zhang, Z.; Ma, J.; Tian, Y.; Wen, L. P.; Jiang, L. A Biomimetic Multi-Stimuli-Response Ionic Gate Using a Hydroxypyrene Derivation-Functionalized Asymmetric Single Nanochannel. *Adv. Mater.* **2014**, *26*, 6560−6565.

DOI: 10.1021/acsami.7b01774
ACS Appl. Mater. Interfaces 2017, 9, 11272−11278